Transport and Communications Science Journal, Special Issue (04/2025), 384-393

Transport and Communications Science Journal

TWO – MODE OVERMODULATION TECHNIQUE FOR INVERTER IN RAILWAY VEHICLE DRIVE SYSTEMS

Pham Van Tien*, Mai Van Tham

University of Transport and Communications, No 3 Cau Giay Street, Hanoi, Vietnam

ARTICLE INFO

TYPE: Research Article
Received: 21/02/2025
Revised: 26/04/2025
Accepted: 28/04/2025
Published online: 30/04/2025
https://doi.org/10.47869/tcsj.76.2025.2

* *Corresponding author*
Email: vantienpham@utc.edu.vn; Tel: +84978319258

Abstract. Source voltage inverters in railway vehicle drive systems often use space vector over modulation techniques in order to enhance the utilization capability of DC voltage. As a result, this can lead to the expansion of the operating range of traction motors. In this paper, the writer does research on a two-mode space vector over modulation technique based on the superposition principle between limit trajectories which are applied to two-level voltage source inverters. The advantage of this technique is the ability to maintain linear control in the over modulation region, which results in low harmonic content in the output AC voltage. In addition, due to its simple control algorithm, it is easy to digitize. The accuracy and the effectiveness of the over modulation technique are demonstrated by both theoretical analysis and simulation results. The research results indicate that this over modulation technique is an efficient option when applied to source voltage inverter control in railway vehicle drive systems.

Keywords: over-modulation, space vector pulse width modulation, two-level voltage source inverter, drive system, railway vehicle.

1. INTRODUCTION

At present, the inverter in the electric drive system of railway vehicles commonly uses a two-level voltage source. Due to constraints on power loss and heat dissipation, the switching frequency of power electronic devices typically does not exceed 1 kHz. However, the output voltage frequency of the inverter supplying the traction motor can exceed 200 Hz. Therefore, a segmented modulation model is generally applied. Two modulation techniques are used: Sinusoidal Pulse Width Modulation (SPWM) and Space Vector Pulse Width Modulation (SVPWM), with SVPWM being more widely adopted nowadays due to its advantages in harmonic elimination and better DC voltage utilization [1, 2]. The SVPWM segmented modulation model integrates multiple SVPWM techniques across the entire operating range of the system [1–3]. These techniques usually include asynchronous modulation applied at low-speed stages, synchronous or segmented synchronous modulation applied at medium-to-high speeds, and six-step modulation applied at high speeds. Within synchronous or segmented synchronous modulation, there are two phases corresponding to two methods: linear SVPWM and overmodulation SVPWM. Overmodulation SVPWM (the inverter's overmodulation region) plays a crucial role in bridging the linear SVPWM phase and the six-step phase.

Research on overmodulation SVPWM techniques for two-level voltage source inverters (VSI) is diverse, with varying complexity and effectiveness [4]. Studies on inverter modulation in the overmodulation region continue to be proposed and refined [5, 6]. In Vietnam, research on using SVPWM for two-level [7], three-level [8], and multilevel inverters [9, 10] has been published. However, studies on overmodulation SVPWM techniques are still limited, particularly in the field of railway transportation.

The two-mode overmodulation SVPWM technique based on the superposition principle between limit trajectories has the advantage of maintaining linear control in the overmodulation region, resulting in low harmonic content in the output AC voltage. Additionally, due to its simple control algorithm, it is easy to digitize [4, 11]. This paper first provides an overview of segmented SVPWM modulation, describes the two-mode overmodulation SVPWM technique based on the superposition principle for two-level voltage source inverters, and then presents simulation results using MATLAB/Simulink.

2. SEGMENTED MODULATION AND SPACE VECTOR OVERMODULATION TECHNIQUE

2.1. Segmented SVPWM modulation

The segmented SVPWM modulation model carries out the inverter modulation process from asynchronous modulation mode to six-step mode. Currently, there are two commonly used segmented PWM modulation models [1], model (I): Asynchronous modulation → Synchronous modulation → Six-step mode, model (II): Asynchronous modulation → Synchronous modulation → Carrier-less modulation → Six-step mode.

Figure 1(a) illustrates modulation model (I). The first stage employs asynchronous modulation, which can utilize either the space vector pulse width modulation (SVPWM) technique or the sinusoidal pulse width modulation (SPWM) technique combined with third-harmonic injection into the sinusoidal modulation wave. The second stage applies synchronous modulation, which includes both the linear modulation region and the overmodulation region. The third stage is the six-step modulation.

Figure 1(b) represents modulation model (II), which differs from the first approach in that it employs carrier-less modulation to transition between the linear modulation region and the six-step mode, rather than using overmodulation for this transition. The fundamental principles of these two methods are essentially the same, except that the optimization objectives differ. In this study, segmented modulation model (I) is used.

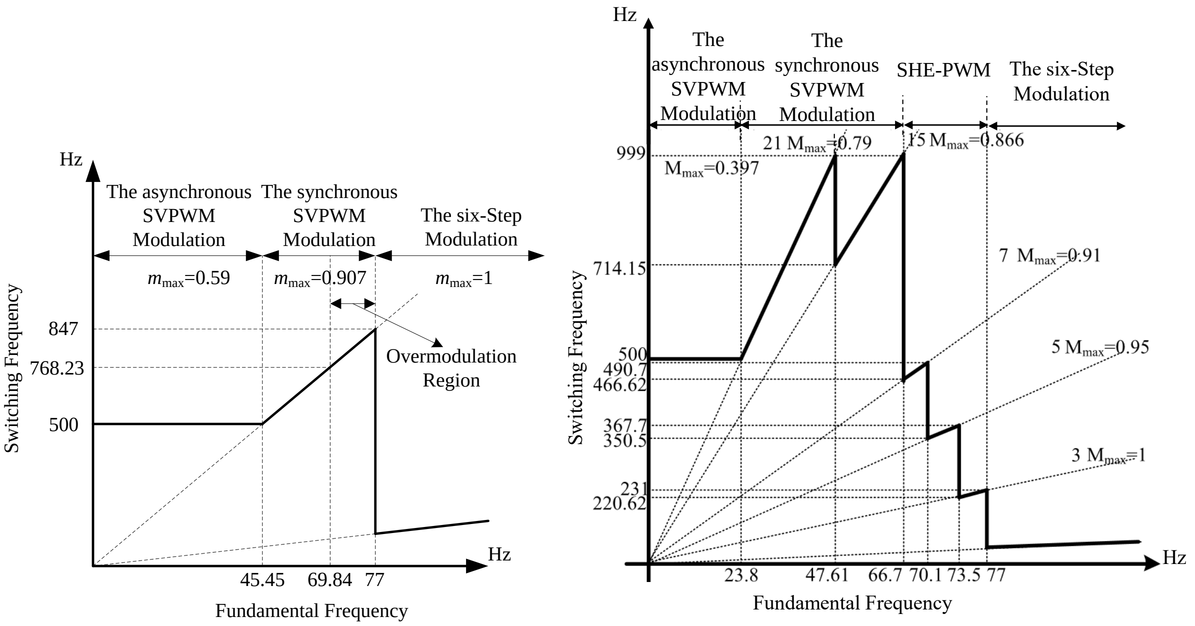

a) b)

Figure 1. Segmented SVPWM modulation Model: a) Model (I); b) Model (II).

2.2. Overmodulation SVPWM based on superposition principle

The circuit diagram of a two-level voltage source inverter (VSI) using IGBT semiconductor switches to supply a three-phase AC traction motor is illustrated in Figure 2. Figure 3 shows the position of voltage vectors generated in the fixed α-β coordinate system, where $\boldsymbol{U}_1$ to $\boldsymbol{U}_6$ (nonzero voltage vectors) have the same amplitude of $2U_{dc}/3$ (U_{dc} is the DC voltage supplied to the inverter), while $\boldsymbol{U}_0$ and $\boldsymbol{U}_7$ (zero voltage vectors) have an amplitude of 0.

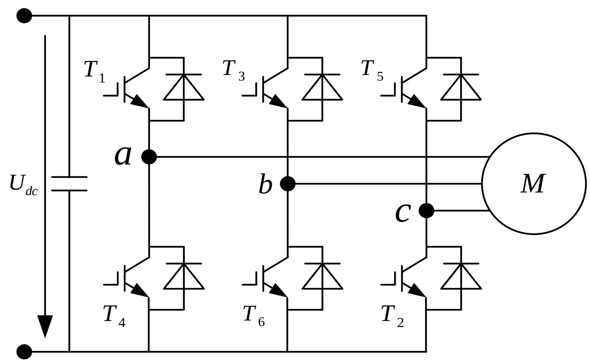

Figure 2. Voltage source inverter – motor circuit diagram.

When the reference voltage vector $\boldsymbol{U}_{ref}$ (the desired output voltage vector of the inverter) belongs to a specific sector, it is synthesized in each modulation cycle T using a linear combination of the right boundary vector $\boldsymbol{U}_{\mathrm{p}}$ and the left boundary vector $\boldsymbol{U}_{\mathrm{t}}$ for durations T_1 and T_2, respectively, as expressed in Equation (1). The remaining time T_0 is allocated to the zero vector. The values of T_1, T_2 and T_0 are determined using Equations (2), (3), and (4).

$$\boldsymbol{U}_{\mathrm{ref}} T = \boldsymbol{U}_{\mathrm{p}} T_1 + \boldsymbol{U}_{\mathrm{t}} T_2 \tag{1}$$

$$T_1 = \frac{2\sqrt{3}}{\pi} mT \sin\left(\frac{\pi}{3} - \theta\right) \tag{2}$$

$$T_1 = \frac{2\sqrt{3}}{\pi} mT \sin\theta \tag{3}$$

$$T_0 = T - (T_1 + T_2) \qquad (T_0 \geq 0) \tag{4}$$

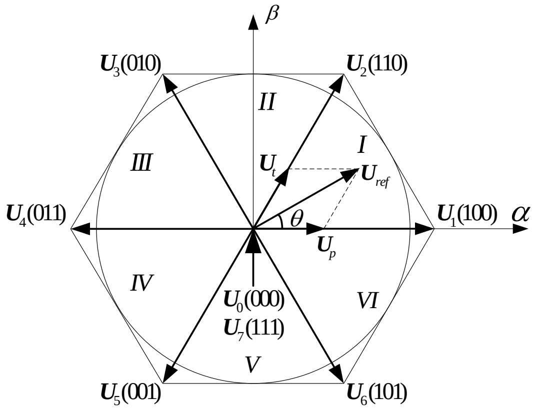

Figure 3. Space voltage vectors.

Where θ is the angle between the reference voltage vector and the right boundary vector, and m is the modulation index, which is calculated using Equation (5).

$$m = \frac{\left|\boldsymbol{U}_{\mathrm{ref}}\right|}{U_{\mathrm{1m\_six\text{-}step}}} = \frac{\left|\boldsymbol{U}_{\mathrm{ref}}\right|}{\left(2U_{\mathrm{dc}} / \pi\right)} \tag{5}$$

Where $\left|\boldsymbol{U}_{\mathrm{ref}}\right|$ is the amplitude of the reference voltage vector, and $U_{\mathrm{1m\_six\text{-}step}}$ is the amplitude of the fundamental harmonic voltage when the inverter operates in six-step mode.

In Figure 3, the hexagonal boundary represents the limit of the reference voltage vector trajectory. The linear modulation region is defined as the area where the trajectory of the reference voltage vector remains circular. This region is bounded by the inscribed circle within the regular hexagon, and the amplitude of the reference voltage vector in this case is $\left|\boldsymbol{U}_{ref}\right| = U_{dc} / \sqrt{3}$, corresponding to a modulation index of m=m_1=0.907. When the modulation index m exceeds m_1, the reference voltage is constrained by the hexagonal boundary, causing the output voltage of the inverter to distort, meaning its actual amplitude is lower than the desired reference voltage. At this point, the inverter enters the overmodulation region. In this region, the overmodulation SVPWM technique is applied by adjusting both the amplitude and phase of the reference voltage, effectively maximizing DC voltage utilization. However, since the control characteristics become nonlinear in the overmodulation region, low-order harmonic distortions appear in the output voltage. These distortions can be linearly compensated using the two-mode overmodulation SVPWM technique, which is based on the superposition principle between limit trajectories.

2.2.1. Overmodulation SVPWM – region I

Due to symmetry, it is sufficient to analyze only one space sector (region I), as shown in Figure 3. Overmodulation region I corresponds to a modulation index in the range: $0.907 \leq m < 0.952$. As illustrated in Figure 4(a), the trajectory of the reference voltage vector $\boldsymbol{U}_{ref}$ is depicted as a thin dashed arc, while the trajectory of the modified reference voltage vector $\boldsymbol{U}_{ref\_I}$ is represented by a bold solid curve. These two vectors differ in amplitude but maintain the same phase angle. This modification ensures that the inverter continues to operate effectively while minimizing harmonic distortion and making optimal use of the available DC voltage.

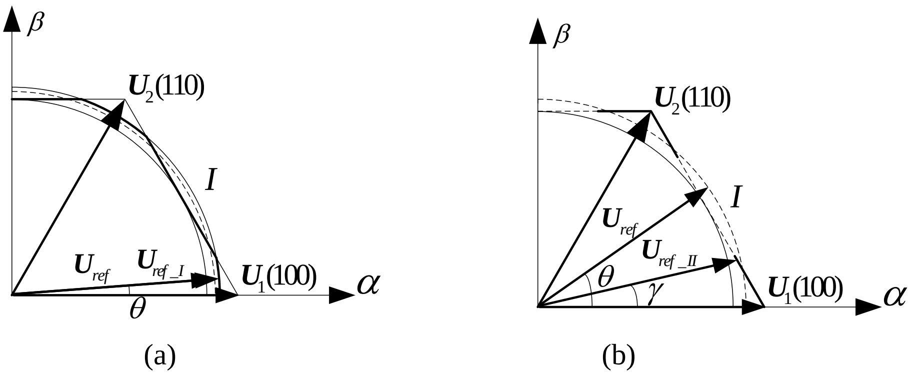

Figure 4. Trajectory of the reference voltage vector in the overmodulation region: a) Overmodulation region I; b) Overmodulation region II.

The correction factor k_1 is defined as:

$$k_1 = \frac{m - 0,907}{0.952 - 0.907} \quad (0 \leq k_1 < 1) \tag{6}$$

Where: When the trajectory of the modified reference voltage vector $\boldsymbol{U}_{ref\_I}$ is the inscribed circle within the regular hexagon, then $k_1 = 0$. When the trajectory of $\boldsymbol{U}_{ref\_I}$ coincides with the hexagonal boundary, then $k_1 = 1$. From Figure 4(a), the inscribed circle within the regular hexagon corresponds to the trajectory of the voltage vector $\boldsymbol{U}_{ref\_I\text{-}sin}$, which represents the sinusoidal modulation limit before entering deeper overmodulation.

$$\boldsymbol{U}_{ref\_I-sin} = \frac{U_{dc}}{\sqrt{3}} e^{j\theta} \tag{7}$$

The regular hexagon corresponds to the trajectory of the voltage vector $\boldsymbol{U}_{ref\_I\text{-}hex}$.

$$\boldsymbol{U}_{ref\_I-hex} = \frac{U_{dc}}{\sqrt{3}\cos\left(\dfrac{\pi}{6} - \theta\right)} e^{j\theta} \tag{8}$$

The trajectory of the modified reference voltage vector $\boldsymbol{U}_{ref\_I}$ lies between the trajectories of $\boldsymbol{U}_{ref\_I\text{-}sin}$ and $\boldsymbol{U}_{ref\_I\text{-}hex}$. Based on the superposition principle, $\boldsymbol{U}_{ref\_I}$ is formed by two components: $\boldsymbol{U}_{ref\_I\text{-}sin}$ with a weighting factor of (1- k_1), $\boldsymbol{U}_{ref\_I\text{-}hex}$ with a weighting factor of k_1.

$$\boldsymbol{U}_{ref\_I} = (1 - k_1)\boldsymbol{U}_{ref\_I\text{-}sin} + k_1\boldsymbol{U}_{ref\_I\text{-}hex} \tag{9}$$

The application times T_1, T_2 of the boundary vectors and T_0 of the zero vector are calculated according to Equations (2), (3), and (4). However, since the expected reference voltage and the actual applied reference voltage are synchronized in phase but differ in amplitude, the modulation index *m* in Equation (5) must be adjusted using the modified reference voltage vector $\left|\boldsymbol{U}_{ref}\right|$ as $\left|\boldsymbol{U}_{ref\_I}\right|$ given in Equation (9).

When the trajectory of the modified reference voltage vector $\boldsymbol{U}_{ref\_I}$ reaches the hexagonal boundary, the modulation index becomes: $m = 0.952$. At this point, the inverter transitions into overmodulation region II.

2.2.2. Overmodulation SVPWM – region II

Overmodulation region II corresponds to the modulation index range: $0.952 \le m < 1$. As shown in Figure 4(b): The trajectory of the reference voltage vector $\boldsymbol{U}_{ref}$ is represented by a thin dashed arc. The trajectory of the modified reference voltage vector $\boldsymbol{U}_{ref\_II}$ consists of discrete bold line segments. These segments gradually shorten as the modulation index *m* increases, indicating that the inverter is increasingly constrained by the hexagonal boundary.

The correction factor k_2 is defined as:

$$k_2 = \frac{m - 0.952}{1 - 0.952} \qquad (0 \le k_2 \le 1) \tag{10}$$

Where: When the trajectory of the modified reference voltage vector $\boldsymbol{U}_{ref\_II}$ forms a regular hexagon, then $k_2 = 0$. When the trajectory of $\boldsymbol{U}_{ref\_II}$ aligns with the boundary vectors (i.e., the vertices of the hexagon), then $k_2 = 1$. In this overmodulation region, to compensate for the portion of the expected reference voltage $\boldsymbol{U}_{ref}$ that cannot be fully achieved, the modified reference voltage vector $\boldsymbol{U}_{ref\_I}$ must remain at the vertices of the hexagon for a certain duration.

The vertices of the regular hexagon correspond to the trajectory of the voltage vector to $U_{ref\_II\text{-}six}$.

$$U_{ref\_II-six} = \begin{cases} \dfrac{2}{3}U_{dc}e^{j\theta}, & 0 \le \theta < \dfrac{\pi}{6} \\ \dfrac{2}{3}U_{dc}e^{j\frac{\pi}{3}}, & \dfrac{\pi}{6} \le \theta < \dfrac{\pi}{3} \end{cases} \tag{11}$$

The trajectory of the modified reference voltage vector $\boldsymbol{U}_{ref\_II}$ lies between the trajectories of $\boldsymbol{U}_{ref\_II\text{-}six}$ and $\boldsymbol{U}_{ref\_I\text{-}hex}$. Based on the superposition principle, the reference voltage vector $\boldsymbol{U}_{ref\_II}$ is formed by two components: $\boldsymbol{U}_{ref\_I\text{-}hex}$ with a weighting factor of $(1 - k_2)$, $\boldsymbol{U}_{ref\_II\text{-}six}$ with a weighting factor of k_2.

$$\boldsymbol{U}_{ref\_II} = (1 - k_2)\boldsymbol{U}_{ref\_I\text{-}hex} + k_2\boldsymbol{U}_{ref\_II\text{-}six} \tag{12}$$

In overmodulation region II, since the actual reference voltage trajectory is still constrained by the hexagonal boundary as described by Equation (12), the switching time calculations still follow Equations (2), (3), and (4). However, at this stage, the expected reference voltage and the actual applied reference voltage differ not only in amplitude but also in phase angle. Therefore: The modified reference voltage vector $\boldsymbol{U}_{ref\_II}$ (from Equation (10)) must be used instead of $\boldsymbol{U}_{ref}$, The corrected clamping angle γ must be used instead of θ. The corrected clamping angle γ is the angle between the modified reference voltage vector $\boldsymbol{U}_{ref\_II}$ and the right boundary vector, and it is determined by equation (13).

$$\begin{cases} \gamma = \arctan\left(\dfrac{(1-k_2)\left|\boldsymbol{U}_{ref\_I\text{-}hex}\right|\sin(\theta)}{(1-k_2)\left|\boldsymbol{U}_{ref\_I\text{-}hex}\right|\cos(\theta)+k_2\left|\boldsymbol{U}_{ref\_II\text{-}six}\right|} \right) & 0 \le \theta < \dfrac{\pi}{6} \\ \gamma = \arctan\left(\dfrac{(1-k_2)\left|\boldsymbol{U}_{ref\_I\text{-}hex}\right|\sin(\theta)+k_2\left|\boldsymbol{U}_{ref\_II\text{-}six}\right|\sin\left(\dfrac{\pi}{3}\right)}{(1-k_2)\left|\boldsymbol{U}_{ref\_I\text{-}hex}\right|\cos(\theta)+k_2\left|\boldsymbol{U}_{ref\_II\text{-}six}\right|\cos\left(\dfrac{\pi}{3}\right)} \right) & \dfrac{\pi}{6} \le \theta < \dfrac{\pi}{3} \end{cases} \tag{13}$$

3. SIMULATION RESULTS

The study utilizes segmented modulation model (I), as shown in figure 1(a). The input DC voltage of the inverter is: U_{dc}=750 V. The asynchronous traction motor used for simulation has the following parameters: Nominal power: S=1225 kVA, Rated voltage: $U_{đm}$=550 V, Rated frequency: $f_{đm}$=77 Hz, Stator resistance: R_s=0.0324 Ω, Rotor resistance: R_r=0.0072 Ω, Stator leakage inductance: L_{ls}=0.72 mH, Rotor leakage inductance: L_{lr}=0.72 mH, Mutual inductance: L_m=0.01059 H, Number of pole pairs: p_n =3.

Figure 5 presents the simulation results of the AC line voltage waveform u_{ab} at the inverter output, along with the corresponding fundamental voltage component for different modulation indices m in the synchronous SVPWM modulation region, before applying the overmodulation technique. Figure 6 shows the results after applying the overmodulation SVPWM technique, demonstrating the improved voltage utilization and reduced voltage error. The voltage deviation (error) between the expected and actual output voltages is summarized in Table 1.

From Figure 5 and Table 1, the following observations can be made: When the modulation index is in the range 0.907 ≤ m, the voltage waveform remains relatively stable, showing minimal distortion. However, the voltage error (difference between the actual fundamental voltage amplitude and the expected reference voltage) increases as mm increases, becoming significantly larger than in the linear modulation region (m<0.907). Additionally, even when the modulation index reaches m=1, the inverter does not fully transition into six-step mode, meaning further adjustments may be required to maximize voltage utilization.

Table 1. Voltage error of different modulation techniques for various modulation index m values.

Modulation index m	**Expected voltage**	**SVPWM technique**		**Overmodulation SVPWM technique**	
		Actual output voltage	***Voltage error %***	***Actual output voltage***	***Voltage error %***
0.9035	747.2	740.5	0.9		
0.936	774.1	757.3	2.2	764.9	1.2
0.975	806.3	770.7	4.4	803	0.4
1	827	776.7	6.1	826.8	0.02

From Figure 6 and Table 1, it can be observed that when the modulation index 0.907 ≤ m, due to the application of the overmodulation technique, as the modulation index increases, the number of pulses in the voltage waveform decreases, while the pulse width increases. As a result, the output voltage increases, significantly improving the voltage error between the actual fundamental voltage amplitude and the expected reference voltage. Due to the linear control capability in the overmodulation region, the harmonic content in the AC output voltage remains low, which is clearly reflected in the Total harmonic distortion (THD) index. Additionally, when the modulation index reaches m=1, the inverter transitions into six-step mode, which aligns with theoretical analysis, confirming the accuracy and effectiveness of the overmodulation technique in maximizing DC voltage utilization within the inverter system.

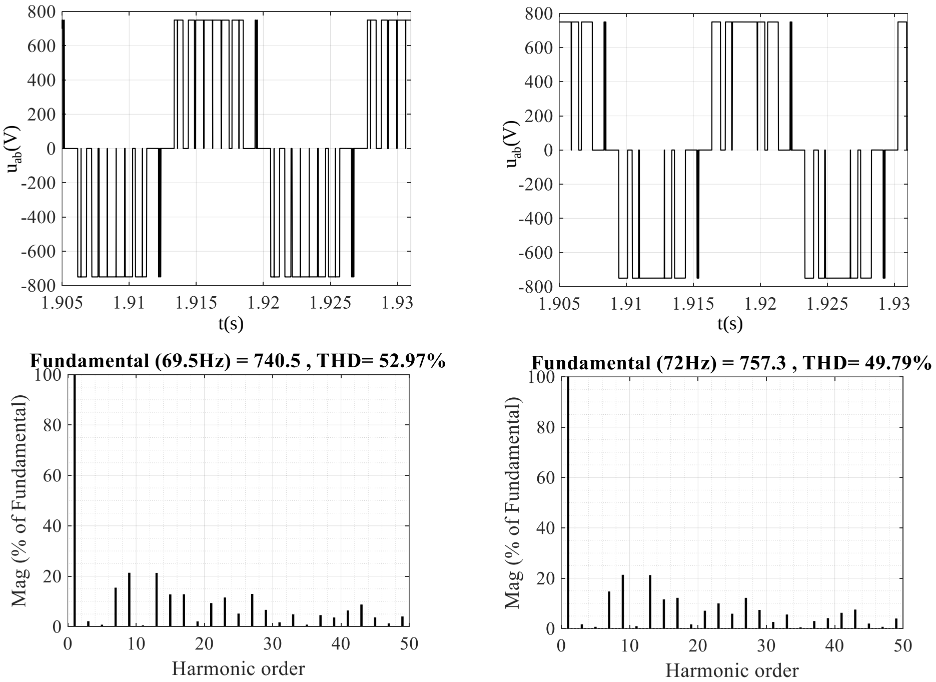

a) m=0.9035, U_{ref} =747.2   b) m=0.936, U_{ref} =774.1

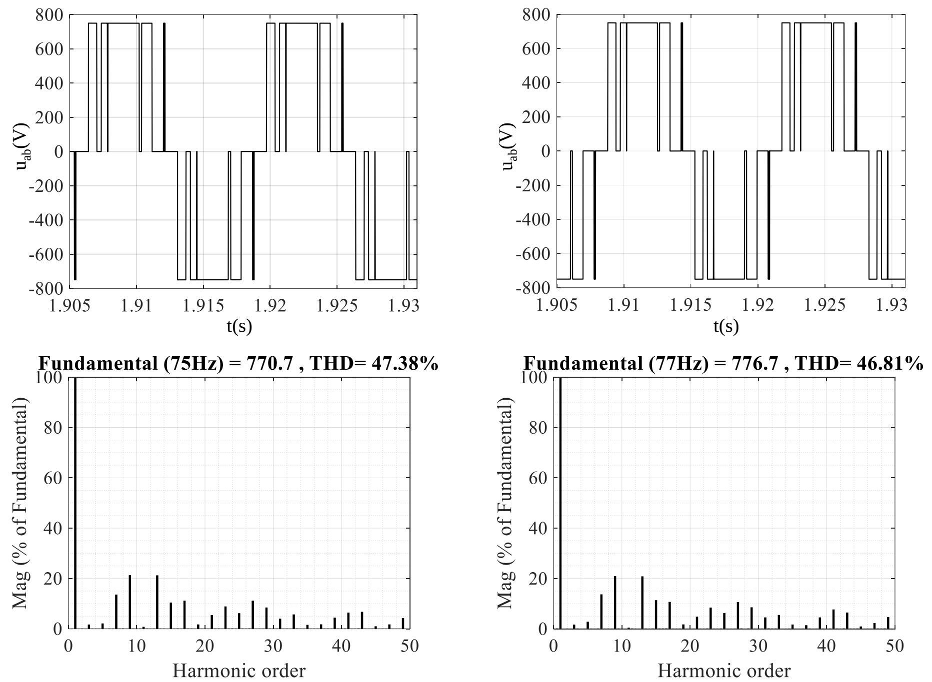

c) m=0.975, U_{ref} =806.3   d) m=1, U_{ref} =827

Figure 5. Simulation results of the SVPWM technique for different mm values.

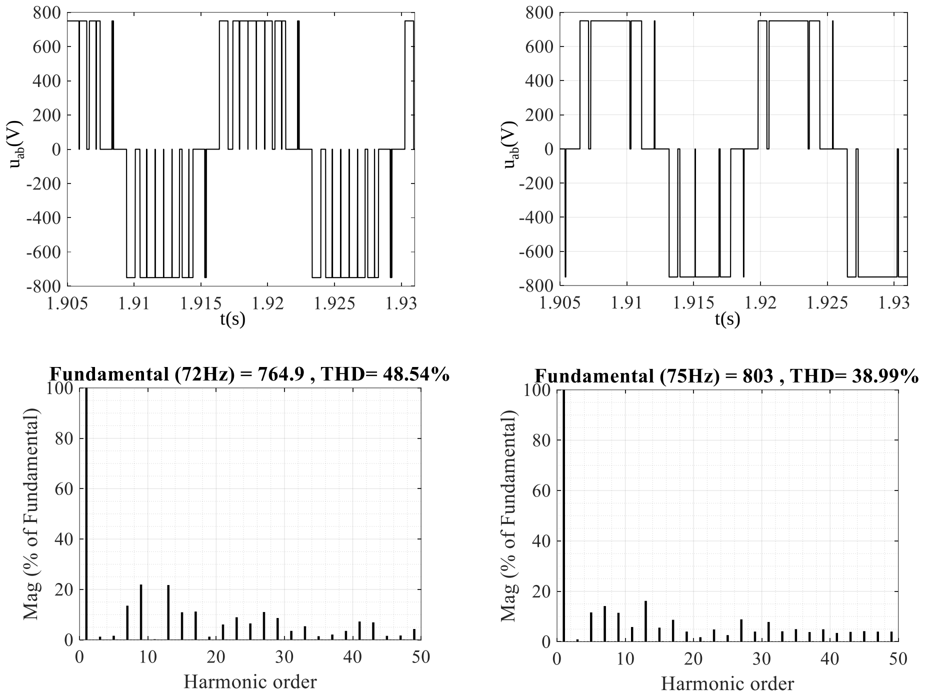

a) m=0.936, U_{ref} =774.1 b) m=0.975, U_{ref} =806.3

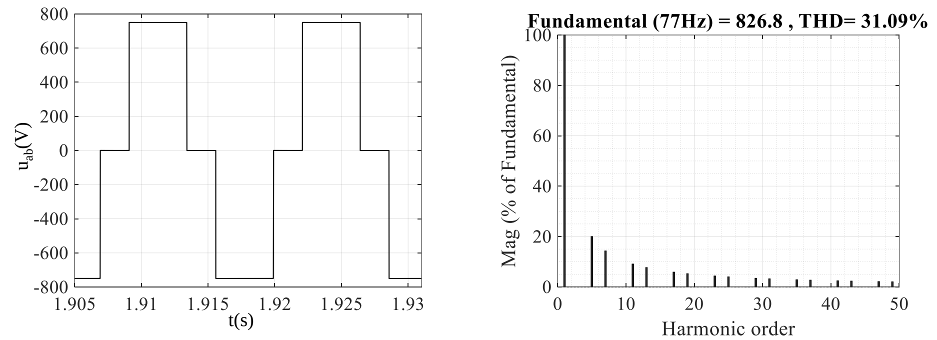

c) m=1, U_{ref} =827

Figure 6. Simulation results of the overmodulation SVPWM technique for different m values.

4. CONCLUSION

In this study, an overview of the SVPWM modulation technique is first presented, followed by a description of the two-mode overmodulation SVPWM technique, which is based on the superposition principle between limit trajectories. Subsequently, simulations are conducted in Matlab/Simulink, utilizing a segmented modulation model combined with the application of the SVPWM technique to the inverter in the railway vehicle drive system. The simulation results demonstrate the accuracy and feasibility of the proposed overmodulation SVPWM technique.

The application of the overmodulation SVPWM technique in inverter control aims to enhance DC voltage utilization, while also serving as a transition mechanism between the linear SVPWM model and the six-step mode. Therefore, the overmodulation SVPWM technique presented in this paper can be effectively applied to two-level voltage source inverters in drive systems that require DC voltage optimization and/or operate in the six-step mode.

REFERENCES

[1]. Jie Chen, Ruizheng Ni, Ting Li Ruichang Qiu, Zhigang Liu, The Harmonic Characteristic of the Advanced Synchronous SVPWM Overmodulation Strategy, IEEE Access, 7 (2019) 148934 – 148949. https://doi.org/10.1109/ACCESS.2019.2946654

[2]. Chen Jie, Li Jun, Qiu Ruichang, Xu Chunmei, Liu Zhigang, Research on space vector PWM synchronous overmodulation in rail transit traction system, Transactions of China Electrotechnical Society, 35 (2020) 91-100.

[3]. Technical design for locomotives and carriages on the Ben Thanh – Suoi Tien route (Line 1), (2015).

[4]. Jin Zhou, Shanhu Li, Jianning Zhang, Tianrui Fang, Xiuyun Zhang, Research on Space Vector Overmodulation Technology of Two-Level PWM Converters, Energies, 15 (2022) 7086. https://doi.org/10.3390/en15197086

[5]. Zisui Zhang, Babak Nahid-Mobarakeh, Ali Emadi, A Simplified Space Vector Overmodulation Strategy for PMSM Drive System, IECON 2022 – 48th Annual Conference of the IEEE Industrial Electronics Society, Brussels, Belgium, 2022. https://doi.org/10.1109/IECON49645.2022.9968949

[6]. Gokhan Altintas, Derya Ahmet Kocabas, Extended Overmodulation Operation of Space Vector PWM for Traction Motor Control at Low Switching Frequency, IEEE Access, 10 (2022) 120274 – 120284. https://doi.org/10.1109/ACCESS.2022.3222082

[7]. Nguyen Van Doai, Quach Duc Cuong, Space Vector Modulation for a Two-Level Three-Phase Inverter on an ARM Cortex Embedded System, Journal of Science and Technology, 53 (2019) 6–13.

[8]. Do Duc Tri, Tran Le Huy, Van Tan Luong, Le Hoang Minh, Space Vector Modulation Technique for a Three-Level Boost Inverter with Total Harmonic Distortion Reduction, Journal of Technical Education Science, 76 (2023) 45-55. https://doi.org/10.54644/jte.76.2023.1305

[9]. Nguyen Thi Thanh Hoa, Ha Duy Thai, Duong Anh Tuan, Mai Van Chung, Generalization of the Space Vector Modulation Method for Cascaded H-Bridge Multilevel Inverters, Journal of Science and Technology, 6 (2021) 3–9.

[10]. Tran Hung Cuong, Pham Viet Phuong, Tran Trong Minh, Space Vector Modulation with an Arbitrary Number of Levels to Optimize Switching Process and Harmonic Components in MMC Multilevel Converters, Measurement, Control, and Automation, 1 (2021) 1-8.

[11]. Fang Hui, Feng Xiaoyun, Ge Xinglai, Song Wensheng, Relationship Studies Between Two-level SVPWM and CBPWM in the Over-modulation Region, Proceedings of the CSEE, 18 (2012) 23-30.